

HVDC grid test models for different application scenarios and load flow studies

Ting AN¹, Congda HAN¹, Yanan WU¹, Guangfu TANG¹



Abstract High Voltage Direct Current (HVDC) grids are the most effective solutions for collection, integration and transmission of large scale remote renewable resources to load centers. A HVDC grid test model can provide a common reference and study platform for researchers to compare the performance and characteristics of a DC grid with different DC control functions and protection strategies. It can also provide reference cases for testing of simulators and digital programs. This paper proposes a comprehensive HVDC grid test model and the associated four sub test models for system studies to meet the research purposes and requirements for different DC grid application scenarios. The design concept, topologies, configurations and functions of the test models are described in detail and their basic system data for load flow studies are provided. Finally load flow simulation studies with PSS/E (Power System Simulator/Engineering) program for each of the models are undertaken and the corresponding results are presented and analyzed in the paper.

Keywords High voltage direct current (HVDC), Line commutated converter-HVDC (LCC-HVDC), Voltage source converter-HVDC (VSC-HVDC), DC grids, Test models

1 Introduction

High Voltage Direct Current (HVDC) grid is a power transmission system which consists of multiple HVDC terminals interconnected through DC lines. The International Council on Large Electric Systems (CIGRE) has given a definition for an HVDC grid as a DC network with a plurality of converters, partially meshed and partially radial [1]. The advantage with a grid is to get increased flexibility and reliability, and to provide redundancy by sharing resources. Comparing to a High Voltage Alternative Current (HVAC) grid, a Voltage Source Converter-HVDC (VSC-HVDC) grid can control its active and reactive power independently and requires less number of circuits for transmission of the same quantity of power. A DC grid can improve the fault-ride through capability and performance of the whole AC system.

With the development and availability of DC circuit breakers, DC–DC converters, DC cables and other relevant technologies [2, 3], VSC-HVDC grids have become possible and are considered to be the most effective technical solutions for the collection and integration of renewable onshore and offshore generation, collection and transmission of remote generation resources to load centers, offshore power supply, etc. Thus, the development of HVDC grids has become an important direction for the future development of smart grids.

HVDC grids are being under research and development (R&D) stages and need to be developed and built gradually. Though a HVDC grid has many advantages, there are

Crosscheck date: 12 May 2016

Received: 19 October 2015/Accepted: 20 May 2016/Published online: 26 July 2016

© The Author(s) 2016. This article is published with open access at Springerlink.com

✉ Ting AN
anting@geiri.sgcc.com.cn

Congda HAN
hancongda@geiri.sgcc.com.cn

Yanan WU
wuyanan@geiri.sgcc.com.cn

Guangfu TANG
gftang@geiri.sgcc.com.cn

¹ Global Energy Interconnection Research Institute, Changping District, Beijing 102211, China

challenges that HVDC grid researchers need to face and deal with, such as how to control power flow and direct voltage and how to achieve fast control and protections. Currently, the researchers around world are undertaking HVDC grids related R&D work with their own models which are of different configurations and data [4–19].

The research results even for the same study scenario could be different and cannot be compared directly and shared effectively if they are not obtained on the same basis. On the other hand, the research funding support for large research projects carried out nationally or internationally tends to be provided by large organizations. Therefore, it is essential and necessary to establish HVDC grid test models to provide unified study platforms and common references for HVDC grid system studies.

In [20–22], the first HVDC test model for studies of different HVDC control strategies was established by Working Group 14.02 of CIGRE Study Committee (SC) 14 in 1991. The CIGRE B4 DC grid test system was proposed by Working Groups B4-58 and B4-57 of CIGRE in 2013 [23, 24]. A brief review and summary of the test model and test system is given in [25].

In [25], a DC grid benchmark model for the application of DC grids for interconnection of two AC systems was proposed. The two independent AC systems are interconnected by a DC grid in the middle. The DC grid is of 13 AC/DC converters, three DC/DC converters to interconnect the three different DC voltage levels of ± 800 kV, ± 500 kV and ± 400 kV, and 18 DC buses. The design concept for the model is to use DC circuit breakers as less as possible to clear DC side faults.

In order to provide common study platforms for different DC grid applications to meet different HVDC grid study purposes and needs, this paper proposes a HVDC grid comprehensive test model (CTM), as shown in Fig. 1. The CTM consists of 3 small HVDC grids and a multi-terminal HVDC (MVDC) system, referred to as Sub Test

Models (STM1 to STM4) which are also defined as DCS-A (DC system A) to DCS-D. The models are designed based on the distribution of China’s renewable energy, existing features and future development trends of the power system in China.

Sections 2–6 in this paper present the four STMs and the CTM respectively in detail with respects to the topology and configuration, and basic system data for load flow studies. The load flow simulation for each of the models with the data and the corresponding results are also presented in these sections. The load flow results confirm the steady state operation of the models. Evaluation of the suitability of the proposed models is given in Sect. 7, and conclusions are summarised in Sect. 8.

The system data proposed are initially for the load flow calculations and can be altered to match the requirements for specific research purposes. The models can also be used for electromagnetic or electromechanical transient studies if typical/common control functions and protection strategies (e.g. those as provided in references [23, 24]) or user defined control functions and protection strategies are implemented to the models.

As the models are designed mainly for studies of DC grids focusing on the performance in the DC side, the corresponding AC systems are represented with simplified systems of AC lines, loads and grid equivalents.

2 Sub Test Model 1 (STM1): DCS-A

China has the favorable conditions for development and construction of large-scale solar, wind and hydro power bases according to the distribution of its renewable energy resources in China. The country is rich in solar and wind, on-shore wind and hydro power resources in the West, North-west and South-west of China respectively, where are the major onshore renewable bases in China. It is also well known that the northern part of China is the coal base which is very much suitable for building clean coal power plants. Therefore a DC grid is proposed based on the energy distribution as shown in Fig. 2 for integration of large scale onshore renewable power generation.

Based on Fig. 2, STM1 or DCS-A on the top left-hand side corner in Fig. 1 is proposed as shown in Fig. 3. In the figure and the other figures, a line drawn represents 3 lines for the AC systems and 2 lines for the DC systems. An onshore AC bus is named as “Ba”, an offshore AC bus as “Bo”, a monopole DC bus as “Bm”, a monopole AC/DC converter as “Cm”, a bipole DC bus as “Bb”, a bipole AC–DC converter as “Cb” and a DC-DC converter as “Cd”.

If specific control functions, protection strategies and proper models of renewable generators are implemented,

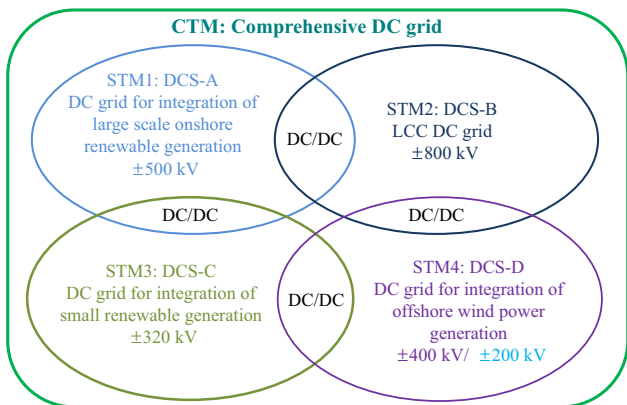


Fig. 1 Relationship of the HVDC grid test models



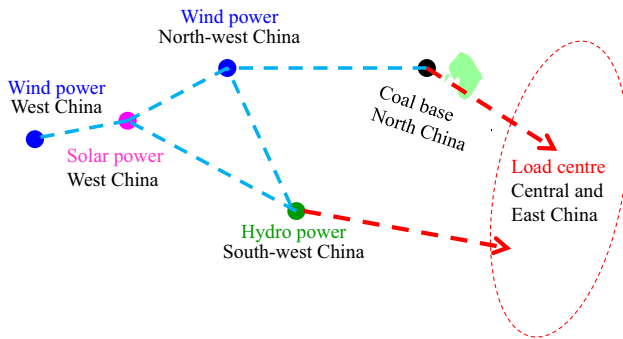


Fig. 2 Sketch of the distribution of China's renewable energy

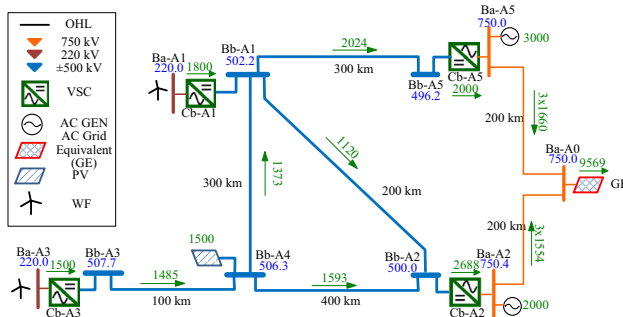


Fig. 3 STM1—DC grid for integration of large scale onshore renewable power generation

STM1 is suitable for electromagnetic transient studies with the converters modeled in detail for designing and verifying the control functions and protection strategies of DC grids. It can be used but not limited to study the complementary characteristics of a DC grid composed with different types of energy resources, to investigate the coordinating control functions, protection strategies and transient performance of the DC grid. The model is suitable for electromagnetic transient studies with the converters modeled in detail for designing and verifying the control functions and protection strategies of DC grids.

2.1 Topology and configuration

DCS-A is a 5-terminal bipolar VSC-HVDC grid and has 5 DC buses as shown in Fig. 3. The 5 DC buses are interconnected via 5 DC overhead lines (OHLs) with the proposed lengths as shown in the figure. The grid has a mesh formed by 3 DC buses of Bb-A1, Bb-A2 and Bb-A4, and two radial branches composed by line Bb-A4 to Bb-A3 and line Bb-A1 to Bb-A5. Two wind farms at Ba-A1 and Ba-A3, one coal fired plant at Ba-A5 and one hydro power plant at Ba-A2 are connected to the DC grid via four AC/DC converters. A solar power plant is connected to the DC bus Bb-A4 directly.

The DC grid collects and transmits the renewable and coal power to an AC system at Ba-A0 via two transmission routes highlighted in orange in Fig. 3. The rest of the AC system is represented by an AC grid equivalent at Ba-A0 which is the slack bus (SB) for the model.

Zhoushan project commissioned in operating in 2014 in China is a 5-terminal radial VSC MTDC system to supply power to islands and to integrate wind power in the islands as shown in Fig. 4 (without the red and yellow dotted lines). The MTDC system can be upgraded to an HVDC grid by adding either the red dotted line or yellow dotted line, resulting in the same topology as STM1.

The benefits of the upgraded DC grids are being of power sharing capability, so as to reduce power losses, provide redundancy and increase the reliability of the grids. Therefore, STM1 can also be used for feasibility studies of extension of the existing MTDC systems to DC grids by adding/removing few lines and/or adjusting the system data to match the actual system data.

2.2 Basic system data for load flow studies

The basic system data proposed for load flow studies for STM1 is summarized in Tables 1–6. As the model is designed for the collection of different types of large scale regional renewable resources, the transmission line lengths are designed within few hundreds of kilometers (100 km to 400 km). Based on the relationships between DC voltages and economic transmission distances, the DC voltage level for the DC grid is designed as ± 500 kV to realize the transmission of power up to 3000 MW [26, 27]. Same logic for determination of DC voltages, transmission distances and amount of power is also applied to the other test models in the paper.

Two AC voltages of 220 kV and 750 kV are marked in brown at buses of Ba-A1 and Ba-A3 and in orange at Ba-A2, Ba-A5 and Ba-A0 respectively as shown in Fig. 3. The

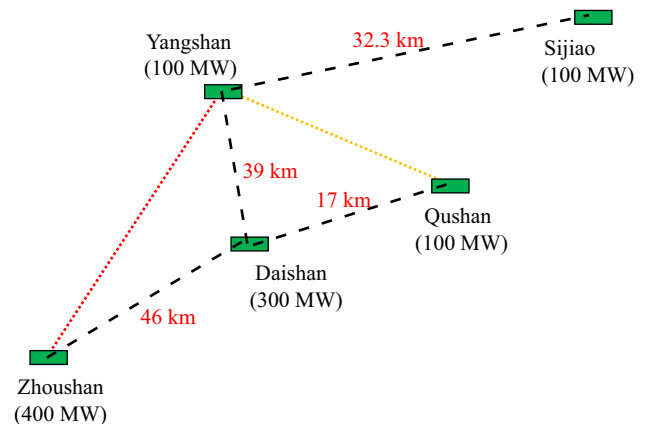


Fig. 4 Zhoushan MTDC system

AC and DC system voltages for all the test models (STM1 to STM4 and CTM) are summarized in Table 1. The bus type, ratings and operating setpoints (settings) of the generators and loads are given in Table 2. Tables 3 and 4 illustrate the AC and DC line data. The AC/DC converter data are listed in Table 5, and the shunt compensator data is given in Table 6.

The ratings of the AC/DC VSCs are determined such that the currents through the electronic devices of VSC are not higher than 2 kA to match the devices’ maximum existing current capability available on the market. This rule is also applicable to the other test models in the paper.

2.3 Load flow simulation and results

A load-flow study is a regime analysis of the electric power flow in an interconnected system. It focuses on the magnitude and phase angle of the voltage at each bus and the real and reactive power flowing in each line for an AC system, or voltage and real power for a DC system. It analyzes the power systems in normal steady-state operation and provides the initial conditions for dynamic simulations, if needed. The load flow results are important for planning future expansion of power systems as well as in determining the best operation of existing systems.

PSS/E (Power System Simulator/Engineering) is a widely used analytical software for electrical power engineering oriented simulations. Its load flow calculation engine can only be directly used for load flow calculations

of AC systems and point to point DC systems, but is not suitable directly for the DC load flow calculations of a DC grid. This paper uses the AC equivalent method for AC load flow calculations of the PSSE to indirectly calculate the DC load flow of a DC grid, i.e., the use of AC components to build an equivalent DC grid system and to calculate the corresponding power flows. The equivalent AC power flow calculated results reflect the DC power flow distributions of the DC grid, so as to realize the function of DC load flow calculations. This method has been verified by modelling the CIGRE B4 DC grid test system mentioned in Sect. 1 and the same load flow results were obtained to those of the test system given in [23, 24].

The test model with the corresponding system data listed in Tables 1–6 was modeled with the PSS/E program. The renewables and loads are modeled as constants without consideration of the variation of renewable sources such as solar and wind generation varying with solar insolation and wind speed.

The PSS/E load flow results for the model are shown in Fig. 3 under setpoint operating conditions (defined as normal operating conditions). Bus voltages in kV are marked in blue and power flow in MW in green with a green arrow line for the direction of power flow. The results show that the renewable power transmitted to the AC system at bus Ba-A0 is approximately 9600 MW. The power flowing through the AC/DC VSCs and lines in the model are shared evenly and all within their ratings. The voltages at all the DC buses are between 0.992 p.u. and 1.014 p.u. which are well within the nominal voltage range of 0.95 p.u. to 1.05 p.u. if a $\pm 5\%$ tolerance is defined practically in the paper.

3 Sub Test Model 2 (STM2): DCS-B

Since the first HVDC project with mercury arc valves and the first HVDC project with thyristor valves were built in 1954 and 1972 respectively, there are approximately 200 HVDC schemes which have been installed, are under

Table 1 System voltages

AC system		DC system	
Color	Voltage (kV)	Color	Voltage (kV)
Dark red	220	Dark blue	± 800
Red	500	Blue	± 500
Orange	750	Purple	± 400
–	–	Dark green	± 320
–	–	Light blue	± 200

Table 2 STM1—system bus data

AC bus					DC bus		
Bus		Generation (MW)		Load (MW)	Bus		Generation/load (MW)
Name	Type	Rating	Setting		Name	Type	
Ba-A0	SB	–			–	–	–
Ba-A1	SB	2500	1800	0	Bb-A1	P	0/0
Ba-A2	PQ	2500	2000	0	Bb-A2	V	0/0
Ba-A3	SB	2500	1500	0	Bb-A3	P	0/0
–	–	–	–	–	Bb-A4	P	1500/0
Ba-A5	PV	3000	3000	0	Bb-A5	P	0/0



construction or in operation around the world. The majority of the HVDC systems are built based on Line Commutated Converter (LCC) technology, i.e. LCC-HVDC technology. This is true for Europe, where most subsea interconnectors use LCC-HVDC technology, although the VSC-HVDC has gained relevance in the last years, and for China where LCC-UHVDC forms the backbone of the power system.

As China's load centers are located at the Central and the East, but the coal bases and renewable resources are mainly located in the West, north-west and south-west of China. There are approximately 2000 kilometers and above between the load centers and energy bases. In order to transmit the power generated with coal and/or renewables, approximately 30 point to point HVDC/ UHVDC schemes based on LCC technology have been built in operation, are under construction or planned in China. Similar growth situation exists in several parts of the world. Therefore, there might be the benefits to form LCC-HVDC grids based on the existing LCC-HVDC schemes to transmit the clean coal fired power and renewable power to the load centers over long distances.

Although most LCC-HVDC schemes in service today are point to point schemes, there are two multi-terminal schemes in service at present, and in these only three converters i.e. terminals are connected together but not forming a mesh. The main reason for limiting the number of LCC-HVDC terminals connected together has traditionally been a result of risk of commutation failures. Another disadvantage with LCC-HVDC for multi-terminal operation is some complexity of power direction changes from import to export or vice versa. In order to achieve power reversal in a LCC-HVDC system, a DC voltage reversal is required resulting in the need of additional switchgear and HV insulation rated at full DC voltage at both ends of the converter.

In order to assess whether a LCC-HVDC grid is feasible, it is necessary to undertake feasibility studies to investigate the technology advantages which could be gained from a LCC-HVDC grid. It also needs to investigate the influences of a LCC-HVDC grid on system reliability and the commutation failure issue, and the new components that are needed to enable a LCC-HVDC grid. Therefore, it is necessary and essential to have a suitable test model for undertaking the feasibility studies.

Table 3 AC line data

AC line (50 Hz)	Resistance R_{AC} (Ω /km)	Reactance X_{AC} (Ω /km)	Susceptance $B_{AC}/2$ (S/km)	Rated current (kA)
500 kV OHL	0.019	0.281	2.03×10^{-6}	3.38
220 kV OHL	0.053	0.305	1.81×10^{-6}	0.71
750 kV OHL	0.013	0.273	2.21×10^{-6}	3.50

Table 4 DC line data

DC line	Resistance R_{DC} (Ω /km)	Rated current (kA)
± 800 kV OHL	0.0062	5
± 500 kV OHL	0.01	3
± 400 kV OHL	0.01	2
± 320 kV OHL	0.01	2
± 400 kV Cable	0.008	2
± 200 kV Cable	0.008	2

Table 5 STM1—AC/DC converter data

Name	Type	Con.	Rating (MW)	Control
Cb-A1	VSC	Bi	2500	$V_{AC} = 1$ p.u., $f_{AC} = 1$ p.u.
Cb-A2	VSC	Bi	5000	$Q = 0$, $V_{DC} = 1$ p.u.
Cb-A3	VSC	Bi	2500	$V_{AC} = 1$ p.u., $f_{AC} = 1$ p.u.
Cb-A5	VSC	Bi	2500	$Q = 0$, $P = 2000$ MW

Note 1. Con.: Configuration, Bi: bipole

2. Power transfer from DC to AC side is positive

3. Converter loss: 1%

Table 6 STM1—fixed shunt data

Bus	Setting (Mvar)
Ba-A2	-600

Note Inductive: negative; capacitive: positive

STM2 i.e. DCS-B on the top right-hand side corner in Fig. 1 is a LCC-HVDC grid and created mainly for carrying out LCC-HVDC feasibility studies as described above. When starting from the existing LCC point to point connections, the model can also be used for the studies on the existing different converter control schemes provided by various manufacturers, and different earthing schemes.

3.1 Topology and configuration

DCS-B as shown in Fig. 5 is a LCC-HVDC grid and designed by interconnecting 2 existing point to point LCC-HVDC schemes (Bb-B1 to Bb-B3 and Bb-B2 to Bb-B4 highlighted in dark blue). The interconnection of the two

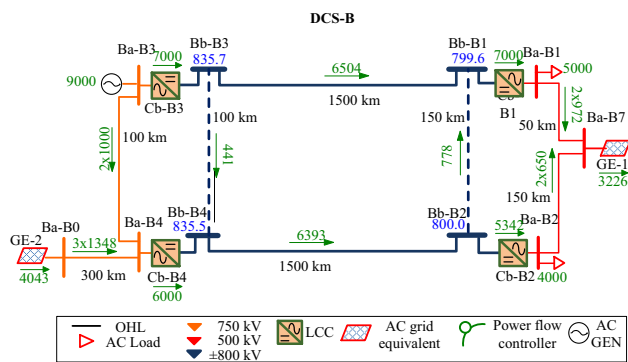


Fig. 5 STM2—LCC-HVDC grid for feasibility studies

schemes is achieved via two DC dashed lines at the both ends in DC side to represent the DC grid formed by the nearby parallel arranged existing schemes.

If the power flow is kept at one direction (e.g. from left to right) the requirement of DC voltage reversal is avoided. For this operating scenario, the AC/DC converters Cb-B3 and Cb-B4 are the rectifiers as power sending ends, and Cb-B1 and Cb-B2 are the inverters as power receiving ends. At the normal operating conditions, the power flows from AC system GE-2 to AC system GE-1 via the DC lines and associated AC lines.

The grid has one DC mesh formed by the 4 DC nodes of Bb-B1 to Bb-B4. If removing any one of the two dashed lines a multi-terminal LCC-HVDC system can also be obtained. The AC systems connected at Ba-B0 and Ba-B7 are represented by two grid equivalents GE-2 and GE-1 respectively, both are slack buses for the model.

3.2 Basic system data for load flow studies

Apart from the data given in Tables 1–6, additional basic system data proposed for load flow studies for STM2 are summarized in Tables 7–9. The rated DC and AC voltages for the grid are ±800 kV highlighted in dark blue and 500 kV in red respectively as shown in Fig. 5. The

Table 7 STM2—system bus data

AC bus					DC bus		
Bus		Generation (MW)		Load (MW)	Bus		Generation/load (MW)
Name	Type	Rating	Setting		Name	Type	
Ba-B0	SB	–	–	–	–	–	–
Ba-B1	PQ	0	0	5000	Bb-B1	P	0/0
Ba-B2	PQ	0	0	4000	Bb-B2	V	0/0
Ba-B3	PV	9000	9000	0	Bb-B3	P	0/0
Ba-B4	PQ	0	0	0	Bb-B4	P	0/0
Ba-B7	SB	–	–	–	–	–	–

Note Load power factor $\cos \psi = 0.95$

Table 8 STM2—AC/DC converter data

Name	Type	Con.	Rating (MW)	Control
Cb-B1	LCC	Bi	8000	$Q = 0, P = 7000$ MW
Cb-B2	LCC	Bi	8000	$Q = 0, V_{DC} = 1.0$ p.u.
Cb-B3	LCC	Bi	8000	$Q = 0, P = -7000$ MW
Cb-B4	LCC	Bi	8000	$Q = 0, P = -6000$ MW

- Note 1. Con.: Configuration; Bi: bipole
- 2. Power transfer from DC to AC side is positive
- 3. VSC loss: 1%, LCC loss: 0.8%

Table 9 STM2—fixed shunt data

Bus	Setting (Mvar)
Ba-B1	1510
Ba-B2	1150
Ba-B4	–710

Note Inductive: negative; capacitive: positive

converter ratings were determined such that the currents through the electronic devices are not higher than 5 kA to match the existing LCC devices current capability available on the market.

The system data (especially the DC voltage of ±800 kV) for the model is based on that of the existing LCC-HVDC schemes in China and it can be adjusted accordingly to that of the existing LCC-HVDC schemes anywhere else.

3.3 Load flow simulation and results

STM2 as shown in Fig. 5 with the corresponding system data listed in Tables 1–9 was modeled with the PSS/E program. The power flow results are illustrated in Fig. 5 for the normal operating conditions. The results show that the power transmitted from left side AC system to the right



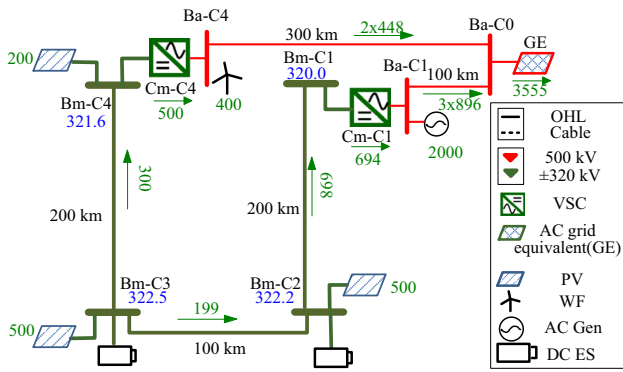


Fig. 6 STM3—DC grid for integration of small renewable power

side AC system is approximately 18 GW. The power flowing through the AC/DC LCCs and DC lines are reasonable, shared evenly and all within their ratings. The voltages at all the DC buses are all between 0.954 p.u. and 1.045 p.u., which are within the nominal voltage range of 0.95 p.u. to 1.05 p.u. if a $\pm 5\%$ tolerance is applied.

4 Sub Test Model 3 (STM3): DCS-C

STM3 i.e. DCS-C is on the bottom left-hand side corner in Fig. 1 and named as VSC-MTDC system. Comparing to STM1, the MTDC system is created for the integration of various smaller onshore renewable generation such as wind power, solar power, hydro-power and energy storage at a lower voltage level (± 320 kV). STM3 can be used to study the feasibility of MTDC system for integration of small scale renewables to increase the penetration of renewable energy into the electricity supply. It also can be used but not limited to investigate the complementary characteristics in space and time between different forms of renewables, coordinating control methods, protection strategies and transient characteristics of MTDC system formed by different types of energy resources if the corresponding control functions and protection strategies are implemented in the model.

Table 10 STM3—system bus data

AC bus					DC bus		
Bus		Generation (MW)		Load (MW)	Bus		Generation/load (MW)
Name	Type	Rating	Setting		Name	Type	
Ba-C0	SB	–	–	–	–	–	–
Ba-C1	PV	2000	2000	0	Bm-C1	V	0/0
–	–	–	–	–	Bm-C2	P	500/0
–	–	–	–	–	Bm-C3	P	500/0
Ba-C4	PQ	600	400	0	Bm-C4	P	200/0

Note Load power factor $\cos \psi = 0.95$

4.1 Topology and configuration

DCS-C is a 4-terminal monopolar VSC-HVDC system as shown in Fig. 6. It has a radial branch formed by four DC terminals Bm-C1 to Bm-C4. A wind power plant is installed at node Ba-C4 and a small hydropower plant or a gas turbine generation at Ba-C1. Three solar power plants are directly connected at the DC buses of Bm-C2 to Bm-C4. Two energy storage plants are also included at Bm-C2 and Bm-C3.

The MTDC system is integrated to the AC system at Ba-C1 and Ba-C4 via two AC/DC converters Cm-C1 and Cm-C4. An AC grid equivalent GE is represented at Ba-C0 which is the slack bus for the model. At the normal operating conditions, the renewable power connected to the MTDC system is transferred to the AC system via the two converters and two AC transmission lines.

4.2 Basic system data for load flow studies

The additional basic system data proposed for load flow studies for STM3 are summarized in Tables 10–12. The DC voltage is ± 320 kV as highlighted in dark green in Fig. 6, whereas the AC voltage is 220 kV.

4.3 Load flow simulation and results

STM3 in Fig. 6 with the corresponding system data was modeled with the PSS/E program. The load flow results are illustrated in Fig. 6. The results show that the renewable power transmitted to the AC system is approximately 3555 MW. The power flowing through the AC/DC VSCs and lines are reasonable and within 60 % of their ratings. The voltages at all the

Table 11 STM3—fixed shunt data

Bus	Setting (Mvar)
Ba-C4	–300

Note Inductive: negative; capacitive: positive

Table 12 STM3—AC/DC converter data

Name	Type	Con.	Rating (MW)	Control
Cm-C1	VSC	Mono	1200	$Q = 0, V_{DC} = 1.0$ p.u.
Cm-C4	VSC	Mono	1200	$Q = 0, P = 500$ MW

Note 1. Con.: Configuration; Mono: monopole
 2. Power transfer from DC to AC side is positive
 3. VSC loss: 1%, LCC loss: 0.8%

DC buses are between 1.00 p.u. and 1.008 p.u., well within the nominal voltage range defined in the paper.

5 Sub Test Model 4 (STM4): DCS-D

STM4 i.e. DCS-D is on the bottom right-hand side corner in Fig. 1 and named as the DC grid for collection and integration of offshore wind power. The DC grid is designed for collecting offshore wind power, supplying offshore load (e.g. oil or gas platform) and integrating them to the onshore AC system. STM4 can be used for offshore DC grid planning and system studies to investigate coordinating control methods, protection strategies and transient characteristics of offshore DC grids if the corresponding control functions and protection strategies are implemented in the model.

5.1 Topology and configuration

DCS-D is a 7-terminal monopole (could be bipolar on needs) VSC-HVDC grid as shown in Fig. 7.

The grid has 3 DC meshes, two DC radial branches, and a few DC-AC mixed meshes. It connects the offshore wind power at buses Bo-D1 to Bo-D4 and Bm-D8 s. A DC energy storage device is also connected at Bm-D8 s. An AC offshore load is connected at Bo-D5.

The offshore power is connected to the onshore DC buses at Bm-D6 and Bm-D7, and then transferred the power to the inland AC system at Ba-D0 via two AC lines. The rest of the AC system is represented by a grid equivalent at Ba-D0 which is also the slack bus for the model.

Both DC overhead lines and DC cables are proposed for the grid to be able to take the possible interactions of those different line types into account.

5.2 Basic system data for load flow studies

The additional basic system data proposed for load flow studies for STM4 is summarized in Tables 13–16. Two DC voltages are proposed for the model and they are ± 400 kV marked in purple and ± 200 kV in light blue respectively as shown in Fig 7. The two DC voltage systems are

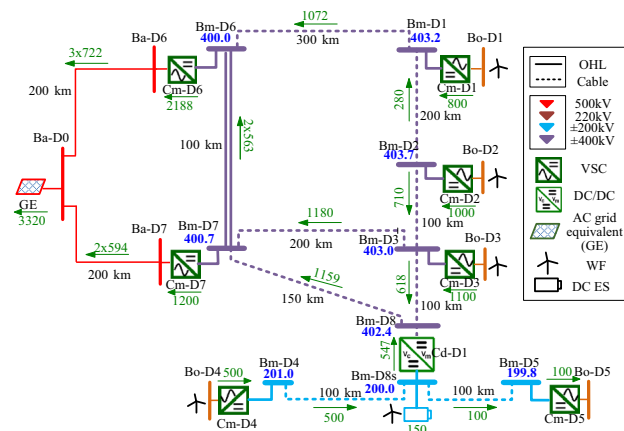


Fig. 7 STM4—DC grid for integration of offshore wind power

interconnected via the DC/DC converter (Cd-D1). The inland AC system voltage is 500 kV and the voltage at offshore AC buses for connecting the wind power plants and the DC load is 220 kV.

5.3 Load flow simulation and results

SBM4 in Fig. 7 with the corresponding system data was modeled with the PSS/E program. The load flow results are illustrated in the figure for the normal operating conditions. The results show that the offshore power transmitted to the onshore AC system is approximately 3320 MW. The power flowing through the AC/DC VSCs and lines are reasonable and within 85 % of their ratings. The voltages at all the DC buses are between 0.999 p.u. and 1.005 p.u., well within the nominal voltage range.

6 Comprehensive test model (CTM)

The HVDC grid Comprehensive Test Model (CTM) is a large HVDC grid formed by the four sub test models addressed above. It covers different applications of DC grids to meet the needs for different research purposes. Due to its large size and complexity, it is not suitable for electromagnetic transient studies. It is designed for electromechanical studies with the converters simplified and modeled with their control functions and protection strategies. The model can be used for the following studies (but not limited to):

- 1) DC grid planning study
- 2) Design and verification of power flow controllers
- 3) Design and verification of DC grid system coordination control functions
- 4) Study of the impact of AC system faults on the operation of the DC grids



Table 13 SBM4—system bus data

AC bus					DC bus		
Bus		Generation (MW)		Load (MW)	Bus		Generation/load (MW)
Name	Type	Rating	Setting		Name	Type	
Ba-D0	SB	–	–	–	–	–	–
Bo-D1	SB	1300	800	0	Bm-D1	P	0/0
Bo-D2	SB	1300	1000	0	Bm-D2	P	0/0
Bo-D3	SB	1300	1100	0	Bm-D3	P	0/0
Bo-D4	SB	700	500	0	Bm-D4	P	0/0
Bo-D5	SB	0	0	100	Bm-D5	P	0/0
Ba-D6	PQ	0	0	0	Bm-D6	V	0/0
Ba-D7	PQ	0	0	0	Bm-D7	P	0/0
–	–	–	–	–	Bm-D8	P	0/0
–	–	–	–	–	Bm-D8 s	V	150/0

Note Load power factor $\cos \psi = 0.95$

Table 14 SBM4—AC/DC converter data

Name	Type	Con.	Rating (MW)	Control
Cm-D1	VSC	Mono	1300	$V_{AC} = 1 \text{ p.u.}, f_{AC} = 1 \text{ p.u.}$
Cm-D2	VSC	Mono	1300	$V_{AC} = 1 \text{ p.u.}, f_{AC} = 1 \text{ p.u.}$
Cm-D3	VSC	Mono	1300	$V_{AC} = 1 \text{ p.u.}, f_{AC} = 1 \text{ p.u.}$
Cm-D4	VSC	Mono	700	$V_{AC} = 1 \text{ p.u.}, f_{AC} = 1 \text{ p.u.}$
Cm-D5	VSC	Mono	150	$V_{AC} = 1 \text{ p.u.}, f_{AC} = 1 \text{ p.u.}$
Cm-D6	VSC	Mono	3200	$Q = 0, V_{DC} = 1.0 \text{ p.u.}$
Cm-D7	VSC	Mono	1600	$Q = 0, P = 1200 \text{ MW}$

Table 15 SBM4—DC/DC converter data

Name	Rating (MW)	Voltage (kV)		Setting
		HV	LV	
Cd-D1	800	±400	±200	$V_{DC}(LV) = 1.0 \text{ p.u.}$

Note 1. HV: high voltage; LV: low voltage

2. Power transfer from HV to LV is positive

Table 16 SBM4—fixed shunt data

Bus	Setting (Mvar)
Ba-D6	–270
Ba-D7	–200

Note Inductive: negative; capacitive: positive

- Study of the impact of DC system faults on the operation of the DC grid
- Design and verification of DC grid fault protection strategies

Apart from the first two studies, the other studies listed above need the corresponding control functions and protection strategies to be implemented in the model.

6.1 Topology and configuration

As shown in Fig. 8, the CTM is composed by 22 DC terminals, 17 AC/DC converters, 5 DC/DC converters and 5 DC voltages (±200 kV, ±320 kV, ±400 kV, ±500 kV and ±800 kV). The 5 DC/DC converters are proposed mainly to interconnect the five DC voltage systems. The DC/DC converters can also have power flow control functions to control the power flowing through the corresponding circuits.

DCS-A is interconnected with DCS-C via the DC line from Bb-A3 to Bb-C4s, with DCS-B via DC double transmission lines between Bb-E1 and Bb-E2, DC/DC converter of Cd-A1 and the AC system at Ba-A0. DCS-B is inter-connected with DCS-D via the DC circuit from Bb-B2 to Bm-D6 and the AC line from Ba-B0 to Ba-D6. DCS-C and DCS-D are interconnected through two routes: one is the DC line from Bm-C1 to Bm-D7 via the DC/DC converter of Cd-C1, and the other is via the AC circuit between Ba-C1 and Ba-D6.

DCS-A, DCS-C and DCS-D are designed as energy generation centers, whereas the two AC systems represented by GE-1 and GE-2 are energy consumption centers. DCS-B with the associated AC lines plays the role of power transmission routes from the energy centers to the power consumption centers.

Three AC system voltage levels of 220 kV, 500 kV and 750 kV are proposed for the CTM. The AC voltage 220 kV is used for the AC buses connected to all the renewable and conventional power plants, whereas the 500 kV and

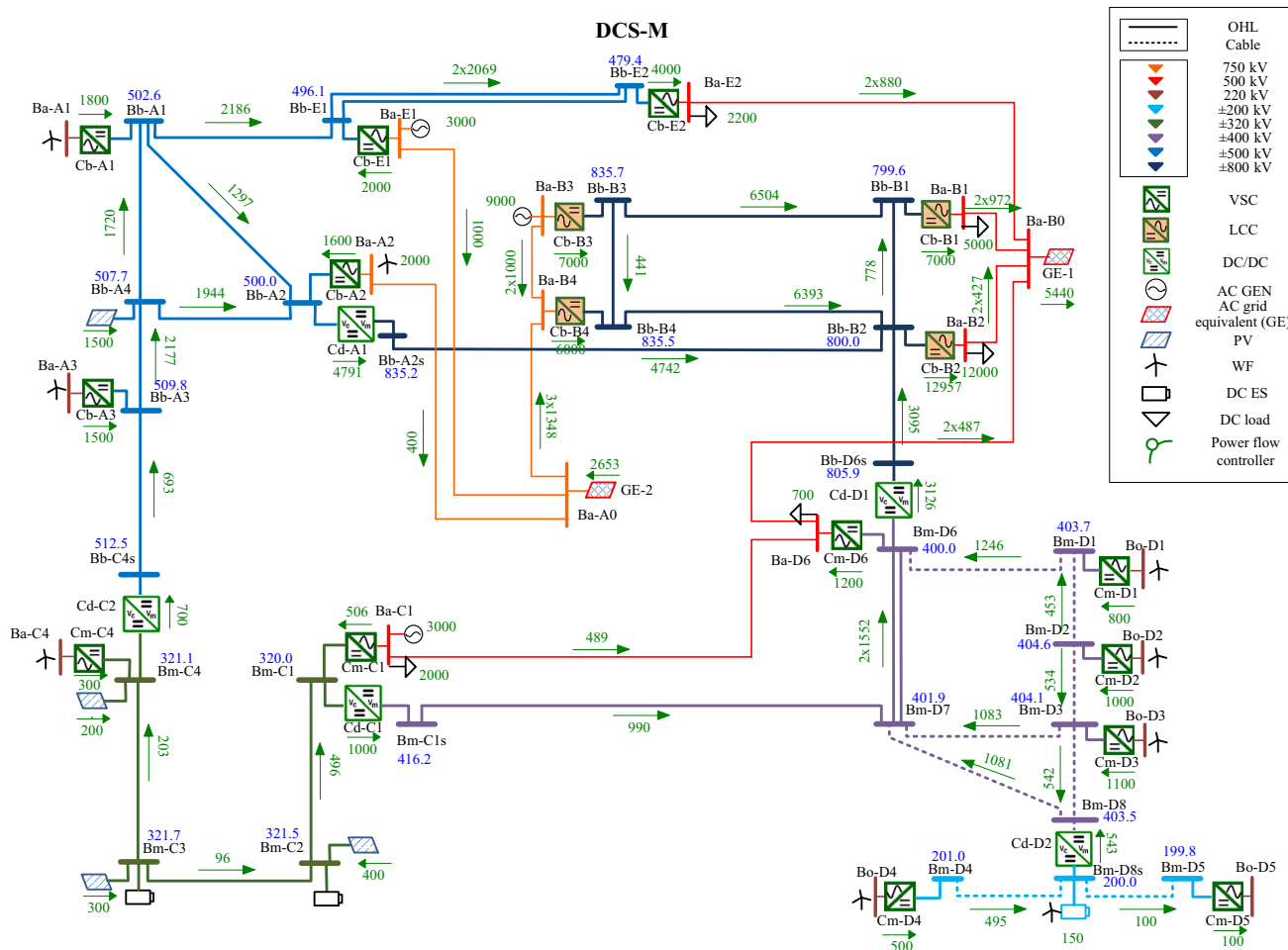


Fig. 8 CTM—comprehensive test model and load flow results

750 kV are for the equivalent AC systems as shown in Fig. 8. Apart from the AC buses connected to all the power plants, all the other AC buses are connected to the two AC systems of 500 kV and 750 kV. One is represented by the grid equivalent of GE-1 at Ba-B0 located at the top right-hand side in Fig. 8 and the other is by grid equivalent GE-2 at node Ba-A0 located in the middle left-hand side.

Normally there is a converter transformer between the AC and DC systems. The required AC voltage for a certain DC voltage can be achieved by correctly specifying the AC voltage at converter side of the converter transformer.

The LCC converters in Fig. 8 can be replaced by VSC converters with the same ratings if a pure VSC DC grid is aimed.

6.2 Basic system data for load flow studies

The most data for load flow studies for CTM is the same as that for DCS-A to DCS-D and can be found from Tables 1–16. The data which are different from that in the tables are highlighted in blue in Tables 17 and 18 and the

additional basic system data is summarized in Tables 17–20.

6.3 Load flow simulation and results

The CTM as shown in Fig. 8 with the corresponding system data was modeled with the PSS/E program. The power flow results are illustrated in Fig. 8 for normal operating conditions.

The results show that the power flowing through the AC/DC VSCs and DC lines are shared evenly and within their ratings. The voltages are controlled between 0.954 p.u. and 1.041 p.u., within the nominal voltage range assumed.

7 Evaluations of the proposed models

The aim of the test models proposed is to provide common study platforms for different DC grid application scenarios and to meet different HVDC grid study purposes. Four different typical common application scenarios of DC



Table 17 CTM—AC/DC converter data

Name	Type	Con.	Rating (MW)	Control
Cb-A2	VSC	Mono	2500	$V_{AC} = 1 \text{ p.u.}, f_{AC} = 1 \text{ p.u.}$
Cb-E1	VSC	Mono	2500	$Q = 0, P = -2000 \text{ MW}$
Cb-E2	VSC	Mono	5000	$Q = 0, P = 4000 \text{ MW}$
Cb-B2	LCC	Bi	16000	$Q = 0, V_{DC} = 1.0 \text{ p.u.}$
Cm-C4	VSC	Mono	600	$V_{AC} = 1 \text{ p.u.}, f_{AC} = 1 \text{ p.u.}$
Cm-D6	VSC	Mono	1600	$Q = 0, P = 1200 \text{ MW}$

Note 1. Con.: configuration; Bi: bipole; Mono: monopole
 2. Power transfer from DC to AC side is positive
 3. VSC loss: 1%, LCC loss: 0.8%
 4. Bold—Different from the data shown in Tables 5–14

grids have been considered by the four Sub Test Models (STM1 to STM4) as presented above. The comprehensive test model (CTM) integrates these four applications to form a comprehensive application of DC grids. Therefore the 5 test models plus the model for interconnection of power systems addressed in [25] can be considered as appropriate to meet the most DC grid application scenarios.

Normally, dynamics in power system are caused by the variations of power demand or different types of disturbances (e.g. faults). Power system studies are using computing simulation software to model and simulate the power system so as to study the steady state power flow and influences of the dynamics upon the power system. From a system study point of view the dynamics are divided into two kinds of simulations, i.e. electromagnetic transient and electromechanical transient simulations.

Table 18 CTM—system bus data

AC bus					DC bus		
Bus		Generation (MW)		Load (MW)	Bus		Generation/load (MW)
Name	Type	Rating	Setting		Name	Type	
Ba-E1	PV	3000	2000	0	Bb-E1	P	0/0
Ba-E2	PQ	0	0	2200	Bb-E2	P	0/0
Ba-B2	PQ	0	0	12000	Bb-A2 s	P	0/0
Ba-C1	PV	3000	3000	2000	Bb-D6 s	P	0/0
Ba-C4	PQ	600	300	0	Bm-C2	P	400/0
Ba-D6	PQ	0	0	700	Bm-C3	P	300/0
					Bm-C1 s	P	0/0

Note Bold—different from the data shown in Tables 2–14

Table 19 CTM—DC/DC converter data

Name	Rating (MW)	Voltage (kV)		Setting
		HV	LV	
Cd-A1	6000	±800	±500	$V_{DC}(LV) = 1.0 \text{ p.u.}$
Cd-C1	1200	±400	±320	$P = -1000 \text{ MW}$
Cd-C2	1200	±500	±320	$P = -700 \text{ MW}$
Cd-D1	4500	±800	±400	$V_{DC}(LV) = 1.0 \text{ p.u.}$
Cd-D2	800	±400	±200	$V_{DC}(LV) = 1.0 \text{ p.u.}$

Note 1. HV: high voltage; LV: low voltage
 2. Power transfer from HV to LV is positive

Table 20 CTM—fixed shunt data

Bus	Setting (Mvar)
Ba-A2	-260
Ba-B4	-720
Ba-E2	550
Ba-B1	1510
Ba-B2	3770

Note Inductive: negative; capacitive: positive

When the power system is disturbed, the initial performance of the system is electromagnetic transients in a very short time period, followed by electromechanical transients. The characteristic of the electromagnetic transients is of high frequency oscillations caused by the exchange of electromagnetic energy stored in the inductors and

capacitors. With the high frequency oscillations dying out, the power system enters to the low frequency oscillation period, i.e. electromechanical transient process.

Due to the high frequency oscillations, the electromagnetic transient simulations are in the range of a few milliseconds to a few hundreds of milliseconds requiring then very small integration time steps (in the range of nanoseconds to microseconds). Thus, the simulations are time-consuming and usually performed for reduced scale power systems. As the electromechanical transients have much lower oscillating frequency than those of the electromagnetic transients the electromechanical transient simulations are in the range of seconds up to minutes with running much larger time steps (milliseconds). Thus, the simulations are much less time-consuming and usually suitable for large scale power systems.

The four different test models as described in the above relevant sections are designed as small as possible to suit for electromagnetic transient studies and large enough to meet the specific application scenarios of DC grids. Due to its size, the offshore DC grid (i.e. STM4) can also be used for the electromechanical transient studies. The comprehensive test model (CTM) is the largest model proposed and should only be used for electromechanical transient studies.

The load flow study belongs to the electromechanical transient simulations range, at special operating conditions without any disturbances (i.e. oscillation frequency = 0 Hz or steady state regime). It analyzes the power systems in normal steady state operation and provides the initial conditions for dynamic simulations. The load flow study has been performed for all five test models to evaluate the suitability of the proposed models. The results show that the power flowing through each of the lines and converters in the models are shared evenly and reasonable, and the voltage at each of the buses is within the nominal voltage range between 0.95 p.u. and 1.05 p.u.. Based on these models, different types of dynamic studies for different applications can be performed accordingly with the control functions and protection strategies modelled.

8 Conclusions

The HVDC grid comprehensive test model (CTM) and the associated four sub test models (STMs 1 to 4) have been proposed to meet the most DC grid research purposes for different DC grid applications. STM1, STM3 and STM4 are proposed for the grid integration of renewables for different DC grid application scenarios. STM2 is a LCC HVDC grid for feasibility studies. STM1 to STM4 are suitable for electromagnetic transient studies whereas the

comprehensive test model CTM as well as STM4 are suitable for electromechanical transient studies

The purpose of the models is to provide common research platforms/references for DC grid studies. The suitability and feasibility of the proposed configurations and basic system data for load flow studies for the models under normal operating conditions have been verified by PSS/E load flow studies. The study results are presented which confirm the steady state operation validity of the models.

Acknowledgment This work was supported by the State Grid Corporation of China, through the 1000-Plan project (No. [2014]264).

Open Access This article is distributed under the terms of the Creative Commons Attribution 4.0 International License (<http://creativecommons.org/licenses/by/4.0/>), which permits unrestricted use, distribution, and reproduction in any medium, provided you give appropriate credit to the original author(s) and the source, provide a link to the Creative Commons license, and indicate if changes were made.

References

- [1] CIGRE WG B4.52 (2013) HVDC Grid Feasibility Study, CIGRE technical brochure 533, Paris
- [2] Tang GF, He ZY, Pang H (2014) R&D and application of voltage sourced converter based high voltage direct current engineering technology in China. *J Modern Power Syst Clean Energy* 2(1):1–15. doi:10.1007/s40565-014-0045-3
- [3] Xiang W, Hua Y, Wen JY et al (2014) Research on fast solid state DC breaker based on a natural current zero-crossing point. *J Modern Power Syst Clean Energy* 2(1):30–38. doi:10.1007/s40565-014-0050-6
- [4] Barker CD, Whitehouse RS (2012) A current flow controller for use in HVDC grids. In: Proceedings of 10th International Conference on AC–DC Power Transmission, London, pp 1–5
- [5] Bucher MK, Franck CM (2014) Comparison of fault currents in MT HVDC grids with different grounding schemes. In: IEEE PES general meeting, National Harbor, conference exposition, pp 1–5
- [6] Bell K, Cirio D, Denis AM (2010) Economic and technical criteria for designing future off-shore HVDC grids. In: Proceedings of IEEE PES innovative smart grid technologies conference Europe (ISGT Europe), pp 1–8
- [7] Beerten J, Cole S, Belmans R (2014) Modeling of multi-terminal VSC HVDC systems with distributed DC voltage control. *IEEE Trans Power Syst* 29(1):34–42
- [8] Wiget R, Andersson G (2012) Optimal power flow for combined AC and multi-terminal HVDC grids based on VSC converters. In: Proceedings of IEEE power and energy society general meeting, pp 1–8
- [9] Veilleux E, Boon TO (2011) Power flow analysis in MT HVDC grid. In: Proceedings of IEEE power systems conference and exposition (PSCE), pp 1–7
- [10] Haileselassie TM, Uhlen K (2013) Power system security in a meshed North Sea HVDC grid. *Proc IEEE* 101(4):978–990
- [11] Akhmatov V, Callavik M, Franck CM (2014) Technical guidelines and prestandardization work for first HVDC grids. *IEEE Trans Power Deliv* 29(1):327–335



- [12] Leterme W, Tielens P, De Boeck S, Van Hertem D (2014) Overview of grounding and configuration options for meshed HVDC grids. *IEEE Trans Power Deliv* 29(6):2467–2475
- [13] Haileselassie TM, Uhlen K (2013) Power system security in a meshed North Sea HVDC Grid. *Proc IEEE* 101(4):78–990
- [14] Wang WY, Barnes M (2014) Power flow algorithms for multi-terminal VSC-HVDC with droop control. *IEEE Trans Power Syst* 29(4):1721–1730
- [15] Wood TB, Macpherson DE, Banham HD, Finney SJ (2014) Ripple current propagation in bipole HVDC cables and applications to DC grids. *IEEE Trans Power Deliv* 29(2):926–933
- [16] Atighechi H, Chiniforoosh S, Jatskevich J, Davoudi A, Martinez JA et al (2014) Dynamic average-value modeling of CIGRE HVDC test system. *IEEE Trans Power Deliv* 29(5):2046–2054
- [17] Egea-Alvarez A, Bianchi F, Junyent-Ferre A, Gross G, Gomis-Bellmunt O (2013) Voltage control of multiterminal VSC-HVDC transmission systems for offshore wind power plants: design and implementation in a scaled platform. *IEEE Trans Ind Electron* 60(6):2381–2391
- [18] Silva B, Moreira CL, Leite H (2014) Control strategies for AC fault ride through in multiterminal HVDC Grids. *IEEE Trans Power Deliv* 29(1):395–405
- [19] Beerten J, Cole S, Belmans R (2014) Modeling of multi-terminal VSC HVDC systems with distributed DC voltage control. *IEEE Trans Power Syst* 29(1):34–42
- [20] Szechtman M, Wess T, Thio CV (1991) First test model for HVDC control studies, CIGRE WG 14.02. *Electra* 135:54–73
- [21] Szechtman M, Wess T, Thio CV (1991) A test model for HVDC system studies. In: *Proceedings of international conference on AC–DC power transmission*, pp 374–378
- [22] Szechtman M, Margaard T, Bowles JP (1994) The CIGRE HVDC test model—a new proposal with revised parameters, CIGRE WG 14.02. *Electra* 157:61–66
- [23] Vrana TK, Yang YT, Jovicic D (2013) The CIGRE B4 DC grid test system, CIGRE WG B4.58. *Electra* 270:10–19
- [24] CIGRE Technical Brochure 604 prepared by SC B4 Working Group B4.57 (2014) Guide for the Development of Models for HVDC Converters in a HVDC Grid
- [25] An T, Zhou XX, Han CD, Wu YN, He ZY, Pang H, Tang GF (2015) A DC grid benchmark model for studies of interconnection of power system. *CSEE J Energy Syst* 1(4):101–109
- [26] Liu ZY (2012) *Electric power and energy in China*. China Electric Power Press, Beijing, pp 161–172
- [27] An T, Yue B, Yang P, Fan Z (2016) A Determination Method of DC Voltage Levels for DC Grids. *Proc CSEE* 36(11):2871–2879

Ting AN received her B.Sc. degree from Xi'an Jiaotong University, China in 1982, the M.Sc. degree from Graduator School of China Electric Power Research Institute (CEPRI) in 1985, and the Ph.D. degree from University of Manchester (former UMIST), United Kingdom in 2000. Currently, she is a Chief Expert in System Design for Smart Equipment at Global Energy Interconnection Research Institute (GEIRI) of State Grid Corporation of China (SGCC), recruited under China's "1000-Elite Program", the recruitment program of global experts sponsored by the Chinese State Council. She is a Chartered Engineer in the UK, a fellow of the IET and a fellowship assessor for the IET. She is a convener of CIGRE B4.72 WG and a guest professor of Institute of Electrical Engineering, Chinese Academy of Sciences. Her research interests are R&D research on VSC-HVDC and HVDC Grids.

Congda HAN received his B.S. degree in electrical engineering from Qsinghua University, in 2010, the M.Sc. degree in power electronics from China Electric Power Research Institute in 2014. Currently, he is an electrical engineer of GEIRI of SGCC. His research interests include the system modeling and analysis of DC grids.

Yanan WU received her B.S. degree in electrical engineering from Zhengzhou University, in 2004, the M.Sc. degree from Beijing Jiao Tong University In 2007, and the Ph.D. degree from China Electric Power Research Institute in 2012, both in power electronics. Currently, she is an electrical engineer of GEIRI of SGCC. Her research interests include the system design and analysis of DC grids in particular.

Guangfu TANG obtained his B.Sc. degree in 1990 from Xi'an Jiaotong University, China, and his Ph.D. degree in 1996 from Institute of Plasma Physics, Chinese Academy of Sciences (ASIPP), both in electrical engineering. He is a professor of CEPRI and a vice president for GEIRI of SGCC. Dr. Tang was the Convener of CIGRE SC B4-48 WG in 2007 and is a member of the IEEE/PES Narain Hingorani FACTS and Custom Power Award Committee. His major research fields are applications of LCC-HVDC, VSC-HVDC and R&D of DC grids.